Proceedings Paper:

Andrews, GE orcid.org/0000-0002-8398-1363, Sattar, H, Heuscar-Medina, C et al. (4 more authors) (2016) Dust Explosions: Recent Developments Including Pulverised Biomass Plenary Lecture. In: Gao, W, (ed.) Proceedings of the 11th International Symposium on Hazards Prevention and Mitigation of Industrial Explosions. 11th International Symposium on Hazards Prevention and Mitigation of Industrial Explosions, ISHPMIE, 2016, 25-29 Jul 2016, Dalian, China. ISHPMIE .

Gordon E. Andrews, Hamed Sattar, Clara Heuscar-Medina, David M. Slatter, Mohammed A. Saeed, Herodotos N. Phylaktou and Bernard M. Gibbs (2016). Dust Explosions: Recent Developments Including Pulverised Biomass. Proceedings of the 11th International Symposium on Hazards, Prevention and Mitigation of Industrial Explosions, 11th ISHPMIE, 24-29, July, 2016, Dalian, China. Plenary Lecture. Prof. G.E. Andrews. Paper ISH004.

Recent Developments Including Pulverised Biomass

Gordon E. Andrews, Hamed Sattar, Clara Heuscar-Medina, David M. Slatter,
Mohammed A. Saeed, Herodotos N. Phylaktou & Bernard M. Gibbs

E-mail: profgeandrews@hotmail.com

School of Chemical and Process Engineering, University of Leeds, UK

Abstract

Dust explosion minimum explosion concentration, MEC, and mixture reactivity measurement are reviewed in terms of the mixture equivalence ratio, Ø, rather than the concentration units of g/m^3, used in all reported dust explosion data. Existing data for MEC implies that HCO dusts are flammable to Ø ~ 0.2, which is leaner than pure hydrocarbon dusts or gases where the MEC is Ø = 0.45. Biomass dusts have a HCO elemental composition and they also show very lean MEC at Ø~0.2. Peak explosion pressure, P_{max}, and the explosion reactivity, K_{st}, are high for a wide range of very rich Ø for many dusts including biomass and this behaviour is different to that in gaseous explosions. The laminar burning velocity, U_L, of dusts was derived from the measured K_{st} and the ISO $1m^3$ explosion vessel can be modified to enable spherical flame speeds to be determined for dusts, which gives two techniques to determine U_L. It was shown that K_{st} and K_G are linearly related to U_L if both are measured in the same 1 m^3 explosion vessel. These laminar burning velocities and K_{st} show that most St1 cellulose type dusts are not very reactive, with S_u less than that for gaseous hydrocarbons. The apparent high reactivity of HCO dusts in the MEC data indicates potential problems in the measurement of MEC for dusts. Part of this problem is that in the ISO $1m^3$ dust explosions around half of the dust is left on the bottom of the vessel at the end of the explosion. Thus the usual nominal concentration of dust in g/m^3 is not the concentration that the flame propagated through. This makes the MEC measurement very difficult as the lower the concentration, the lower the proportion of the dust that burns, so that the concentration in the flame front at the MEC is difficult to determine. The Hartmann equipment is potentially a more reliable method of determining the MEC, but this also has its experimental problems, related to whether the injected dust is mixed at ignition. For woody and plant biomass dusts there are additional problems with the fibrous nature of the dusts: the standard dust pot size will not hold sufficient mass and the fibres block in the standard 'C' ring dust injection system. Solutions to both of these problems are demonstrated with new calibrated dust injection systems for fibrous biomass. The wide particle size distribution in biomass dusts is a further problem and experiments show that very coarse woody biomass can explode and a mechanism for this is developed involving the propagation of the flame in the fines with the coarse particles gasifying in the burnt gases of the fine flame. This explains the rich MEC for coarse biomass and the lack of a rich limit.

Keywords: dust explosions, pulverized biomass, industrial explosions.

1. Introduction

Dust explosions are a widespread hazard in process plant powdered chemicals, in agricultural grain storage, in modern biomass pellet production plants and in pulverized biomass preparation and storage plants. This review concentrates on the explosion and flame propagation properties of pulverized biomass and shows the limitations of existing test equipment. In the UK pulverized woody biomass burning in existing coal fired power stations generated 5.7% of electricity in 2014. There is a strong influence of dust particle size on the MEC and mixture reactivity and recent evidence shows that quite coarse sawdust can explode with a high pressure rise but a low mixture reactivity [Wong et al., 2013] and it is shown that this is a common feature of pulverized biomass.

A major factor in explosion safety is the knowledge of how much of a gas, vapour, mist or dust has to be mixed with an oxidant for an explosion to be possible. It will be shown in the next section that if the elemental composition of the dust in known then the stoichiometric (Φ=1) mixture can be calculated and this then enables the lean explosion limit mixture (Φ_{LL}) or minimum explosion concentration (MEC) to be expressed as a multiple of Ø. The minimum ignition energy of gas/air mixtures is <1mJ for most flammable gases and vapours and <10mJ for most mists and <100mJ for most dusts. Thus, the elimination of ignition sources is not the most reliable method of explosion protection, as the energy required is so trivial. However, an ignition source of 10 KJ or more cannot ignite a flammable gas, vapour, mist or dust if the mixture ratio is not in the flammable concentration range and this is the most crucial aspect of explosion protection.

2. Concentration of dust should be A/F by mass and then converted to equivalence ratio, Ø.

The normal way dust/air mixture concentrations are referred to in the literature is g_{dust}/m^3_{air} {Eckhoff, 2003]. The volume of air is at standard or ambient temperature and pressure with a typical air density of 1.2 kg/m^3. Satter et al. (2012) compared dust explosion mixture reactivity, K_{st}, and the peak overpressure, $P_{max}/P_{initial,}$ from the literature at the same g/m^3 concentration, as shown in Fig. 1 (left). Comparison of dust data at the same g/m^3 irrespective of the material is meaningless and can be dangerous, as the concentration with the highest reactivity for one dust may be quite different for another dust. All the dust concentations in Fig. 1 (left) are the mass of dust placed in the external pot of the explosion vessel divided by the volume of the vessel at atmospheric pressure and temperature conditions. This will be referred to as the nominal dust concentration, as it will be shown to not be the concentration of dust that the flame propagates through.

The dust explosion data in Fig. 1 (left). are shown as a function of the nominal equivalence ratio in Fig. 1 (right) and this shows that the most reactive mixture and the peak overpressure for all materials occurs for very rich nominal Ø and this behavior is completely different from that of gases. Also, there is effectively no rich flammability limit for dusts. The cellulose results have a peak reactivity of Ø = 2 and this is twice the concentration expected from gas explosions. Polyethylene is the most difficult result to explain as this is a pure hydrocarbon and the peak reactivity is Ø = ~8.

It is considered that g/m^3 is a poor unit to use for dust concentration as it is only valid for conditions where measurements were determined at ambient conditions, so that the volume is the same in the test method and in the equipment to be protected. However, it cannot be applied if the temperature in the equipment is higher, as there is then less mass of air in unit volume. Nor can it be applied if the dust is in a high pressure facility, as there is more mass of air in unit volume than at atmospheric pressure. This has led to misleading reporting of the influence of temperature and pressure on flammability limits and mixture reactivity for dust mixtures [Eckhoff, 2003; Bartknecht, 1993]. If stoichiometry is always expressed in terms of A/F ratios on a mass basis, mass$_{air}$/mass$_{dust}$, then this confusion cannot arise and confusion in data leads to accidents. Another problem with the g/m^3 dust concentration unit, is that where the mixture is relative to stoichiometric is not known and is generally not discussed in the literature. The mass concentration relative to the stoichiometric concentration is the mixture equivalence ratio, Ø, which is the same as the stoichiometric A/F by mass divided by the actual A/F by mass. The equivalence ratio, Ø, is the mixture concentration unit used in most combustion work on gaseous fuels and should be the method used for mixture concentration in dust explosions.

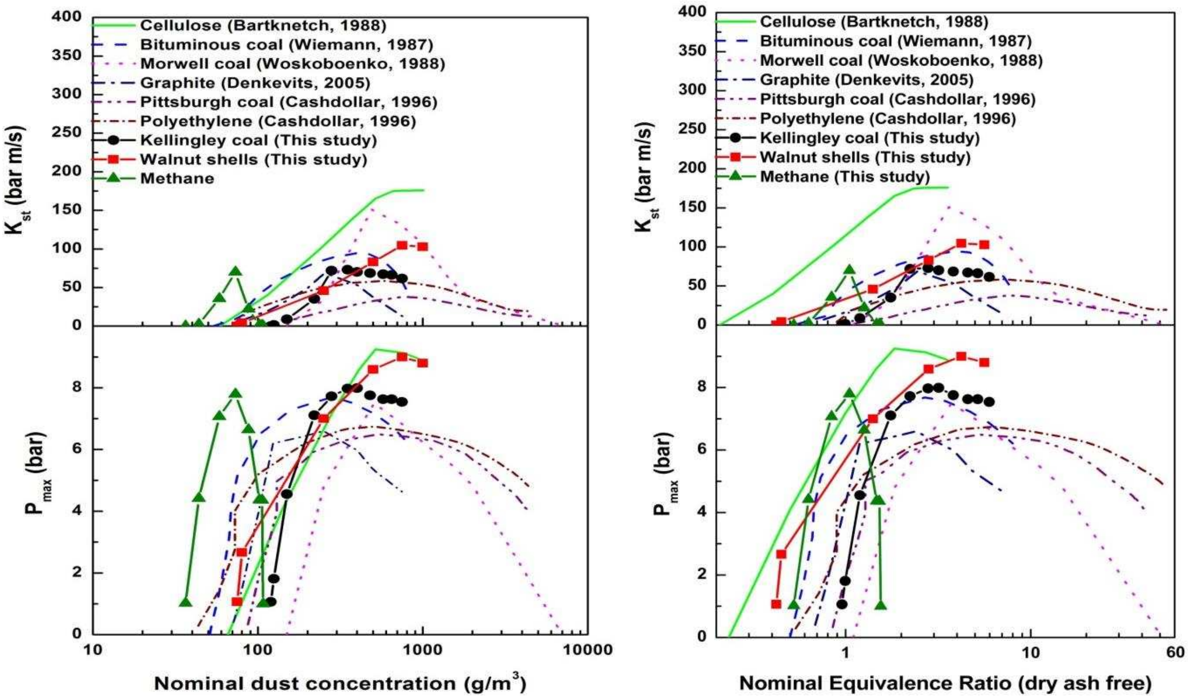

Fig. 1 Literature results for explosion reactivity, K$_{st}$, and overpressure P$_{max}$ as a function of the nominal dust g/m^3 (left) and as a function of the nominal equivalence ratio (right). [Satter et al., 2012]

Most stoichiometry calculations are based on gases and derive the results as volume percent (vol%); this is of little use if there is a mist or dust explosion hazard. These calculation methods are also not applicable to practical liquid fuels, such as kerosene, with hundreds of different hydrocarbons. The only method of explosion stoichiometry which deals with gases, vapours, mists and dust explosion hazards is mass based air/fuel (A/F) ratios. It may be shown [Andrews and Phylakyou, 2010] that the air/fuel ratio by mass for any hydrocarbon (HC) or HCO flammable gas, vapour, mist or dust is given on a dry ash free basis (daf) by Eq. 1.

$$\text{Air/Fuel}_{Mass} = (1 + y/4 - z/2)\ 137.94 / (12 + y + 16z) \qquad (1)$$

Table 1 The stoichiometric A/F by mass for a range of gases, mists and dusts with the lean limit equivalence ratio, Φ_{LL}. Measurement of Φ_{LL} at ambient T and P. [Andrews and Phylaktou (2010).

Material	y	z	A/F $\Phi=1$ daf	% by vol. $\Phi=1$	g/m^3 $\Phi=1$ daf	Φ_{LL} Zabetakis (1965)	Φ_{LL} EN 1839: 2003	LL g/m^3	Φ_{LL} Dust daf
Methane	4	0	17.2	9.5%	69.8	0.53	0.46	37, 32	
Propane	2.67	0	15.7	4.0%	76.4	0.55	0.425	42, 32	
Ethylene	2.0	0	14.8	6.5%	90.2	0.48	0.38	43, 34	
n-hexane	2.33	0	15.2	2.15%	78.9	0.56	0.47	44, 37	
Gasoline	2.0	0	14.8	~2.4%	81.1	0.55 0.60		45 48	
Kerosene	1.95	0	14.7	~1.4%	81.6	0.51		42	
Diesel	1.90	0	14.6	~1.0%	82.1	0.50		41	
Hydrogen			34.5	29.6%	34.8	0.14	0.12	5, 4	
Methanol	4	1	6.47	6.7%	185	0.46		85	
Ethanol	3.0	0.5	9.0	6.51%	133	0.66	0.48	88, 64	
Isopropanol	2.67	0.33	10.39	4.43%	116	0.45	0.45	52	
Acetone	3.0	0.33	9.52	3.9%	126	0.64		81	
Cellulose	1.67	0.83	5.12		234			55 60	0.23 0.25
Hemicellulose	1.17	1.0	3.15		381				
Lignin	1.11	0.22	9.56		126				
PMA	1.50	0.50	7.27		165			30	0.18
PMMA	1.60	0.40	8.28		145			30	0.21
polyethylene	2.0	0	14.8		81			30	0.37
polypropylene	2.0	0	14.8		81			35	0.43
Polyethylene terephthalate (PET)	0.8	0.4	7.18		167			40	0.24
Polyvinyl acetate (PVA)	1.5	0.5	7.22		166			40	0.24
Pitch Pine	1.46	0.42	8.09		148			30-60	0.2-0.4
Spruce	3.58	1.55	3.83		313			20 70	0.06 0.22
Carbon	0	0	11.5		104			60	0.55
Bituminous Coal	0.778	0.073	12.7 9.51		94+ 126			55	0.58 0.44

+ On a dry ash free basis, # 5% water and 20% ash.

Table 2 Stoichiometry and lean flammability limits of metal dust explosions [Andrews and Phylaktou, 2010; Eckhoff, 2003; NFPA68, 2013; Field, 1983]

Metal	MW	$A/F_{Ø=1}$	$g/m^3_{Ø=1}$	Measured LL g/m^3	$Ø_{LL}$
Ca	40	1.73	694	60	0.086
Mg	24	2.88	417	30	0.07
Zn	65	1.06	1130	125 250	0.11 0.22
Cu	63.5	1.09	1101	750	0.68
C	12	11.5	104	60	0.58
Si	28	4.93	243	30	0.25
S	32	4.31	278	30 20	0.11 0.072
Al	27	3.83	313	30-60	0.1-0.2
Fe	56	1.85	649	500 200	0.77 0.31
Cr	52	1.99	603		
U	238	0.43	2759	125 480	0.05 0.17

Table 3 Biomass Dust Samples Compared with Lignite [Wilén, C., A. et al.,1999]

Biomass	MEC daf 1m^3	O/C z	H/C y	Stoich A/F	Stoich g/m^3	MEC Ø daf	Mean Particle Size µm	SOF daf
Wood	29.4	0.731	1.59	5.63	213	0.138	95	83.6
Bark	27.8	0.637	1.42	6.03	199	0.140	57	74.1
Forest Residue	55.3	0.672	1.53	4.78	251	0.220	102	79.5
Spanish Pine	83.1	0.729	1.63	5.69	211	0.394	247	85.0
Barley Straw	72.5	0.705	1.68	5.91	201	0.357	253	78.6
Miscanthus	110.4	0.771	1.62	5.42	221	0.498	143	79.6
Soghum Straw	105.8	0.647	1.45	6.02	199	0.531	178	79.8
Rapeseed Straw	174.5	0.986	1.88	4.54	264	0.661	318	61.4
German Lignite	51.8	0.450	1.09	7.12	169	0.307	58	53.4
Spanish Lignite	59.6	0.826	1.42	4.88	246	0.242	40	55.3

Table 4 Biomass composition analysis and Stoichiometric A/F by mass

Biomass	Labels	Ultimate analysis					Proximate analysis					Bomb cal.	Stoich. calc.	
		C (%)	H (%)	O (%)	N (%)	S (%)	H_2O (%)	VM (%)	VM (%)	FC (%)	Ash (%)	CV (MJ/Kg)	Stoich. A/F	Stoich. A/F Actual
		daf	daf	daf	daf	daf	ar.	ar.	daf	ar.	ar.	actual daf	daf.	(g/g)
Bagasse	B	55.6	7.3	35.7	1.3	0.1	7.2	67.1	92.3	5.6	20.1	15.6 21.5	7.5	5.4
Rice Husk	RH	49.8	6.4	42.7	1.1	0.0	7.7	62.3	83.7	12.2	17.9	15.2 20.4	6.2	4.6
Wheat Straw	WS	50.6	6.4	41.5	1.4	0.1	6.8	60.7	86.2	9.7	22.8	14.5 20.6	6.4	4.5
Corn Cobs	CC	45.9	6.0	46.8	1.2	0.1	7.1	69.4	82.5	14.8	8.8	14.8 17.6	5.4	4.5
Peanut Shell	PS	53.7	6.6	38.2	1.5	0.0	7.00	66.4	78.1	18.6	8.0	18.2 21.4	6.9	5.9
Steam exploded wood	BP	52.8	5.8	41.0	0.4	0.0	4.4	73	78.6	19.9	2.7	19.5 21.0	6.28	5.8
Walnut shell	WAL	52.9	6.8	39.6	0.6	0.1	5.0	74.6	84.0	14.2	6.3	19.2 21.7	6.8	6.0
Pistachio nut shell	PIS	49.4	6.3	41.7	2.6	0.0	2.7	78.4	88.1	10.7	8.3	18.2 20.4	6.2	5.5
Corn flour	CF	44.7	7.4	47.8	0.1	0.0	11.6	77.8	92.0	6.8	3.8	16.4 19.4	5.7	4.8
Lycopodium	LC	68.2	9.4	20.4	2.0	0.0	1.6	89.2	94.6	5.1	4.1	29.6 31.4	10.4	9.8
Oak sawdust	OAK	51.4	6.5	41.8	0.2	0.0	8.9	72.7	84.6	13.3	5.1	20.0 23.3	6.4	5.5
Pine wood mixture	PWP	49.7	7.0	42.6	0.7	0.0	3.5	79.5	90.0	8.7	8.2	19.2 21.7	6.3	5.6
Milk powder	MP	52.4	7.7	35.2	4.4	0.2	4.6	79.2	88.0	10.7	5.4	22.3 24.8	7.5	6.8
Biscuit flour	BIS	40.7	5.6	51.0	2.7	0.0	11	78.4	92.1	6.8	3.9	14.8 17.4	4.5	3.9
SPF wood mixture	SPFR	50.5	7.0	41.4	1.2	0.0	7.8	73.5	82.0	16.2	2.6	18.3 20.4	6.4	5.7
SPF torrified	SPFT	54.7	6.9	37.4	1.1	0.0	4.0	74.6	80.4	18.2	3.2	20.8 22.4	7.1	6.6
Whole tree wood (Raw and torrified)	ECNR	52.9	6.3	40.9	0.0	0.0	5.3	78.0	85.9	12.8	3.9	18.9 20.8	6.5	5.9
	ECNT	52.7	6.2	40.8	0.3	0.0	2.0	78.2	82.6	16.5	3.3	20.1 21.2	6.5	6.2
Wood (Raw and torrified)	RWER	47.0	6.1	44.7	2.2	0.0	4.6	83.4	92.4	6.8	5.1	18.3 20.3	5.8	5.2
	RWET	56.0	6.0	35.2	2.7	0.0	3.9	68.9	78.6	18.8	8.4	20 22.8	7.3	6.4
Norway spruce (Raw and torrified samples at different conditions)	S2SR	53.4	6.2	40.3	0.0	0.0	5.8	79.0	87.7	11.1	4.1	19.2 21.3	6.5	5.9
	S2STS	55.5	5.6	38.1	0.8	0.0	2.8	77.0	82.8	15.9	4.2	21.8 23.4	6.7	6.2
	S2STA	59.9	5.7	33.6	0.8	0.0	2.7	69.4	75.8	22.1	5.8	20.8 22.5	7.5	6.9
	S2STB	58.6	5.3	35.3	0.7	0.0	3.4	63.6	73.6	22.8	10.2	20.0 23.1	7.1	6.1
Southern pine (Raw and torrified)	NBER	52.3	5.8	41.2	0.6	0.0	5.0	78.5	84.9	14.0	2.5	19.4 21	6.3	5.8
	NBET	58.4	5.6	35.2	0.8	0.0	3.3	70.3	76.1	22.1	4.3	21.6 23.4	7.2	6.7
Kellingley Coal	K Coal	82.1	5.2	7.0	3.0	0.1	1.7	29.2	36.9	50	19.1	25.0 31.6	11.6	9.2
Colombian Coal	C Coal	81.7	5.3	9.6	2.6	0.0	3.2	33.7	41.3	47.8	15.3	26.4 32.4	11.2	9.1

where y is the elemental H/C molar ratio in the fuel and z is the O/C molar ratio. The stoichiometric A/F for a range of gases and dusts in the literature in shown in Table 1 as A/F by mass, g/m^3 and for gases and vapours % by volume. This shows that for most hydrocarbons, whether gas, vapours, aerosols or solid dusts the stoichiometric A/F by mass is 14.7-15.7 with only methane higher at 17.4.

For agricultural and biomass dusts there is often ash and absorbed water present. If the A/F by mass stoichiometry is evaluated on the elemental composition on a dry ash free basis (daf)

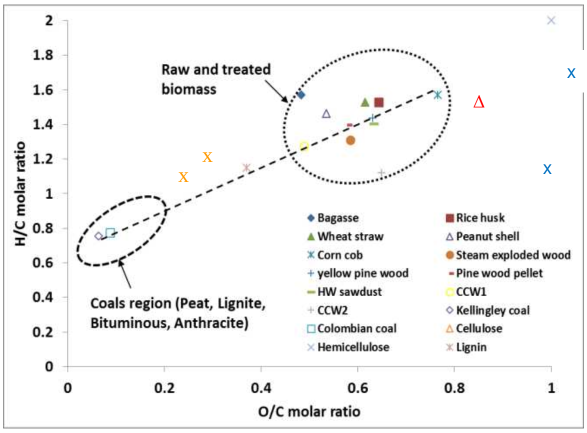

Fig. 2 H/C as a function of O/C for biomass

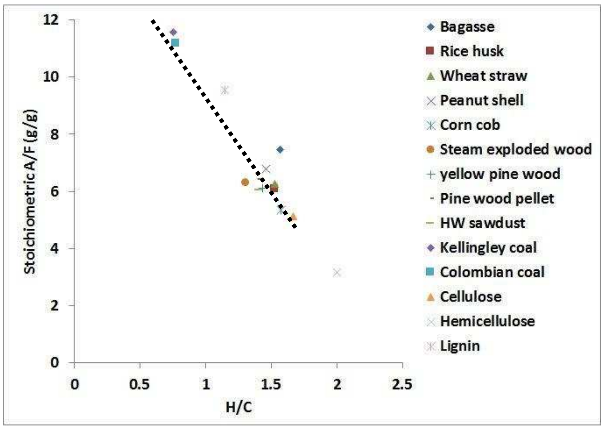

Fig. 3 stoichiometric A/F as a function of H/C

then the actual air/fuel can be calculated from Eq. 2 where the water (w) and ash (a) content are on a mass basis.

A/F by mass = A/F(daf)[1-(w+a)] (2)

For example if the bituminous coal had a typical 5% moisture and 20% ash then the actual A/F by mass would be 9.5/1 (126 g/m^3) instead of the 12.7 on a daf basis.

For metal dust explosions the stoichiometric A/F by mass can be derived [Andrews and Phylaktou, 2010] and these are summarized in Table 2. The higher MW of metals means that the stoichiometric A/F is lower than for HC or HCO materials, but the stoichiometric concentration in g/m^3 is higher than for HC and HCO materials in Table 1.

For pure HCO vapours (alcohols) and solid pure HCO dusts the stoichiometric A/F in Table 1 varies from 6.5 – 9.5, which is a wider range then for hydrocarbons and is the range for alcohols. For solid pure HCO materials (PMA, PMMA, PET and PVA) the range of stoichiometric A/F is from 7.2 – 8.3. For cellulose type dusts (wood) the stoichiometric A/F on a daf basis varies from 3.8 to 8.1 and this is a wider range than for HC or HCO non-cellulose substances. However, the data for biomass in Table 1 is the only data in the classic literature prior to the extensive use of pulverized biomass for power generation purposes. This dearth of explosion data on biomass dusts is because the standard dust explosion test equipment is difficult to use with pulverized woody biomass, due to the fibrous nature of some biomass.

A range of biomass stoichiometry is shown in Table 2, which is based on the biomass elemental analysis of Wilen et al. (1999) which has been used with Eq. 1 to show that the biomass stoichiometric A/F varies from 4.8 – 6.0. A wider range of biomass and torrefied biomass is shown in Table 4 from the authors work, the abbreviation of the biomass in Table 4 are used later in the presentation of explosion results for these biomass.. Table 4 has a range of stoichiometric A/F on a daf basis from 4.5 to 7.5. Lycopodium biomass is unusual with a stoichiometric A/F of 10.4, similar to acetone at 9.5. It is also unusual as a naturally occurring powder (plant pollen used in the perfume industry) with a very fine particle size and is very reactive [Eckhoff, 2003]. It has been extensively used in dust explosion research as it requires no milling, but it is unrepresentative of most biomass which do not naturally occur as a fine powder.

Some of H/C and O/C ratios in Table 4 are plotted as variables in Fig. 2 and there is a reasonable correlation and the data points lie within the trend of other biomass in the literature. The stoichiometric A/F is plotted as a function of H/C in Fig. 3 and there is a good

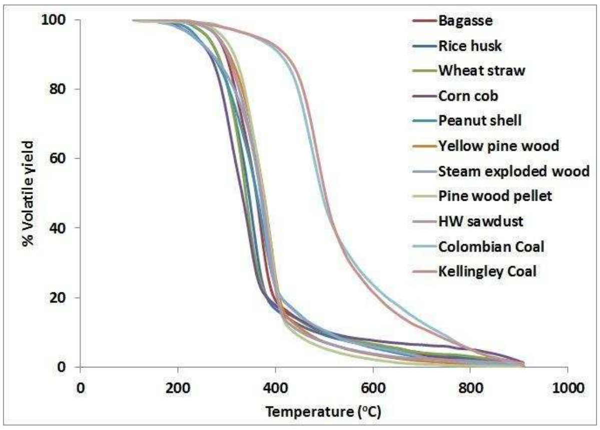

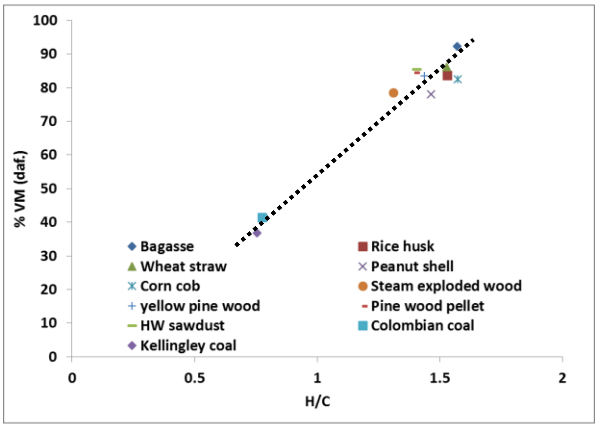

Fig. 4 Volatile release as a function of temperature. Fig. 5 VM% as a function of H/C

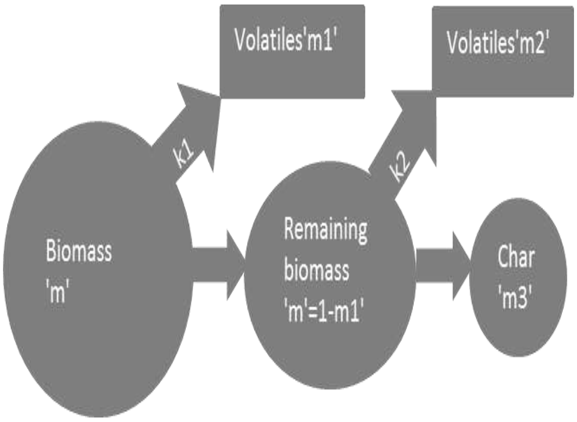

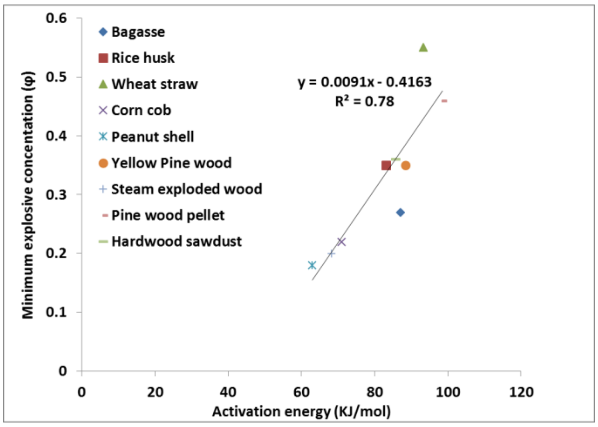

Fig. 6 Staggs (1999) series reaction model for volatile yield from solid polymers.

Fig. 7 Correlation of the MEC with volatile release activation energy from Staggs model.

correlation. Fig. 2 also shows the H/C and O/C of cellulose and three monomers of hemi-cellulose and lignin, which are the constituent polymer stuctures in most biomass. This data does not fit the line for the biomass and shows that each biomass has a different proportion of the natural polymers.

3. Volatile Content of Biomass Dusts

Another feature of biomass dusts is their high volatile content, which is shown in Table 4 to vary from 73.6 to 92.3% daf with lycopodium powder unusually high at 94.6%. This is in contrast to coal with much lower volatile content at around 40%. TGA analysis of the biomass volatiles compared with coal are shown in Fig. 4 and this shows that for biomass the volatiles are released over the temperature range 200-600^{o}C but that 70% of the volatiles are released in the range 300-400^{o}C, which is quite different from coal where 70% of the volatiles are released in the range 450-600^{o}C. Fig. 5 shows that the volatile content is correlated by the H/C and there is a poorer correlation with the O/C. The measurement of the volatile content by thermal gravimetric analysis (TGA) is a slow heating process. It is possible that under fast heating in a flame front, the carbon is converted to CO and adds to the volatiles. This is likely to happen as it is shown later that there is no evidence of the formation of char in the residues after biomass explosions.

Table 5 Comparison of the elemental composition with cellulose, hemi-cellulose and lignin [Tillman, 1981].

Wood	Elemental composition	Stoichiometric A/F	Cellulose	Hemi-cellulose	Lignin
Beech	$CH_{1.94}O_{0.803}$	5.58	45.2%	32.7%	22.1%
White Cedar	$CH_{1.524}O_{0.667}$	5.97	48.9%	20.4%	21.4%
Spruce	$CH_{3.584}O_{1.55}$	3.83	48.5%	21.4%	27.1%

Table 6 Bulk and particle densities with the calculated porosity of biomass samples

	B	RH	WS	CC	PS	BP	YPW	Blz	Dfl	Dk 1	Dk 2
Bulk density (Kg/m^3)	204	382	318	284	320	437	229	199	210	240	196
True density (Kg/m^3)	1671	2203	1702	-	-	1752	1678	1757	1784	1675	1695
Porosity (%)	88	83	81	-	-	75	86	89	88	86	88
BET surface area (m^2/g)	0.96	-	1.96	-	-	1.6	1.55	0.84	1.46	-	-

The Staggs (1999) quick approximation method was used to determine the kinetic data for the rate of volatile's yield from a solid that is applicable for low temperature TGA analysis. Two different models were developed: the Series Reaction Model and the Competitive Reaction Model. The series reaction model is shown in Fig. 6 and Saeed et al. (2015a) have applied this to the present biomass samples in Table 4 and shown that it can predict the activation energy for the release of volatiles using the TGA plots shown in Fig. 3. The results for some of the biomass in Table 4 are shown in Fig. 7, which shows that the minimum explosion concentration (MEC), using the Hartmann method, correlates well with the ease of release of volatiles. There was no improvement in the correlation for the competitive reaction model (Saeed, 2015a).

It was also found that the volatile release activation energy increased with the content of water and ash in the biomass, as shown in Fig. 8. There were two correlation lines with agricultural waste biomass being less sensitive to water and ash and woody biomass being more sensitive. This was found to result in two different trends for the MEC as a function of ash plus moisture, as shown in Fig. 9. This shows that agricultural biomass have the least impact of ash + moisture on the MEC as a result of the lower impact on the activation energy for the release of volatiles. The reason for this is not known, but it shows that the ease of volatile release is crucial in determining the MEC for biomass. It also shows that the main action of ash and water is not just to act as an inert mass that absorbs heat from the flame and reduces the MEC through the lower flame temperature mechanism. This is the action that gives the reduced MEC with increase in water + ash for agricultural dusts in Fig. 9.

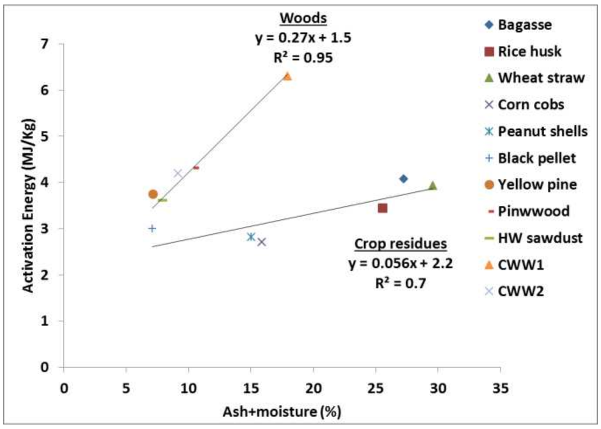

Fig. 8 Increase in the activation energy for volatile release as a function of the ash + moisture mass % of the biomass.

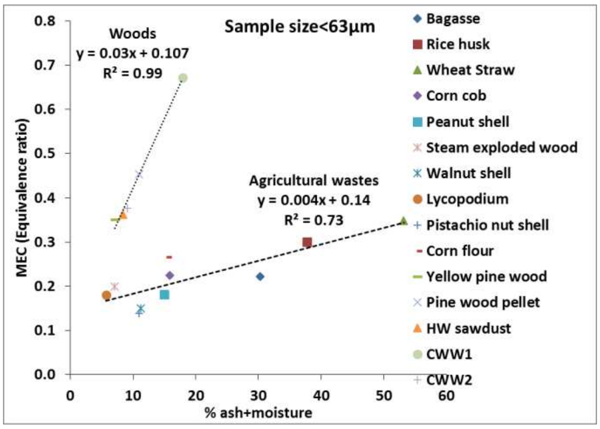

Fig. 9 Influence of the ash + moisture on MEC

Biomass thus contrasts with metal dusts, in that biomass flame propagation is almost entirely through the release of volatiles and metal dusts is through direct oxidation of metal powders. As a consequence biomass dust will propagate a flame for relatively large particle sizes, as discussed later, but metal dust need to be very fine, often < 10µm [Eckhoff, 20013], before they will propagate a flame. However, this is the size range that metal powders are manufactured for the modern process of 3D printing of metal objects and for the control of grain size in metals. Coal may lie between biomass and solid metals in that it is usually modelled as volatile burning followed by char or solid carbon combustion.

The shape of the volatile mass loss as a function of temperature in Fig. 4 is controlled by the proportion of hemi-cellulose (first mass loss in the range 200-300^{o}C), the constant mass loss rate in Fig. 4 is the cellulose decomposition over 300-400^{o}C and the final mass loss is due to lignin over the range 400-900^{o}C. Yank et al. (2006) showed that these temperature ranges overlap as the decomposition range of hemi-cellulose overlaps that of cellulose, which overlaps that of lignin: hemicellulose decomposes 220-315^{o}C, cellulose 315-400^{o}C and lignin >400^{o}C. However, for biomass samples the presence of ash interferes with the release of volatiles, so that precise use of the TGA traces to determine hemi-celulose, cellulose and lignin is difficult. However, they give a rough indication that typically biomass is 25% lignin and hemicellulose and 50% cellulose, but each biomass is slightly different as shown in Fig. 4.

Biomass dusts are in the cellulose class of substances and have a wide range of compositions in the 3.8 – 8.1 A/F range in Tables 1, 3 and 4. Biomass have a range of proportions of hemi-cellulose, cellulose and lignin. There are several monomers of hemi-cellulose and lignin, but the most common of these is given in Table 1. Hemi-cellulose has a stoichiometric A/F of 3.15, with the monomers ranging up to 4.6. Lignin has monomers that range in stoichiometric A/F from 8.2-11.1. It is the range of monomers that give the overlap in the decomposition temperatures of the three components of biomass. There are often similar amounts of hemi-cellulose and lignin in a biofuel and the differences in stoichiometric A/F will cancel out, leaving the overall stoichiometric A/F close to that of cellulose. Fig. 2 shows the H/C as a function of O/C for biomass and for cellulose and for three monomers of hemi-cellulose and lignin. The correlation is roughly linear with variation from the linear due to different proportions and types of hemi-cellulose, cellulose and lignin. A sample high in lignin will be low in O/C and a sample high in hemi-cellulose will be high in O/C, but if they are in similar proportions then the O/C will be close to that for cellulose. Measurements of hemi-cellulose, cellulose and lignin in biofuels are difficult and scarce in the literature. Table 5 shows three woody biomass where data sources exist for the elemental composition and cellulose, hemi-cellulose and lignin [Tillman, 1981], although the elemental composition is from different data sources and will not be the same batch of wood. The results in Table 5 show little relationship between H/C and O/C or stoichiometric A/F and the hemi-cellulose and lignin proportions. However, Table 5 does show that TGA determination of hemi-cellulose and lignin is reasonable with 25% for each and the rest cellulose; this methodology is worth further development.

Sheng and Azevedo (2002) proposed a model to measure the proportions of cellulose, hemicellulose and lignin contents. The proposed correlations were based on H/C, O/C and volatile matter (VM) for a large number of biomass samples with a correlation coefficient of 90% as given by Eqs. 3 and 4.

$$Cellulose = -1019.07 + 293.810\left(\frac{\mathrm{O}}{\mathrm{C}}\right) - 187.639\left(\frac{\mathrm{O}}{\mathrm{C}}\right)^2 + 65.1426(\mathrm{HC}) - 19.3025\left(\frac{\mathrm{H}}{\mathrm{C}}\right)^2 + 21.7448(\mathrm{VM}) - 0.132123(\mathrm{VM})^2 \qquad (3)$$

$$Lignin = 612.099 + 195.366\left(\frac{\mathrm{O}}{\mathrm{C}}\right) - 156.535\left(\frac{\mathrm{O}}{\mathrm{C}}\right)^2 + 511.357(\mathrm{H/C}) - 177.025\left(\frac{\mathrm{H}}{\mathrm{C}}\right)^2 - 24.3224(\mathrm{VM}) + 0.145306(\mathrm{VM})^2 \qquad (4)$$

The inclusion of the VM in the correlation as well as the H/C and O/C is because hemi-cellulose has a high VM and lignin a low VM and a biomass with a high VM contect indicates a high hemi-cellulose composition and a low VM indicates a high lignin content.

Table 6 shows the bulk density and cell wall density determinations of several of the biomass in Table 4. A micromeritics AccuPyc 1330 gas displacement pycnometer was used for the true density measurement. Utilizing these values of densities, the porosity of these solid fuels were also calculated. The results showed a wide difference of actual particle and bulk densities with high porosities. Possible reason for this is highly irregular fibrous structure leaving intra-particle spaces in packing. A Micromeritics Tristar 3000 surface area and porosity analyser was used to determine the BET surface area and the results are given in Table 6. A variation from 0.84-1.96 m^2/g was found. The large surface area and high porosity contribute to the rapid release of volatiles in flame propagation.

4. The composition of the dust mixture that burns in the ISO 1 m^3 vessel

Satter et al. (2012) showed that an important feature of dust explosions in the ISO 1m^3 equipment was that around half of the mass of dust placed in the external pot was left in the vessel at the end of the explosion, usually as a pile of dust at the bottom of the vessel. For sticky dust such as milk powder and sugar the unburnt dust adheres as a layer on the wall and the outer surface is slightly blackened by quenching the flame. Analysis of the debris left after the explosion shows that it has the same composition as the original dust with the same size distribution and is largely unburnt dust that has not participated in the explosion. The mass burnt is shown as a function of the mass injected in Fig. 10. The mass injected is the nominal mass placed in the external dust pot less any mass remaining in the dust pot and connecting pipework at the end of the explosion as this never entered the vessel and could not participate in the explosion.

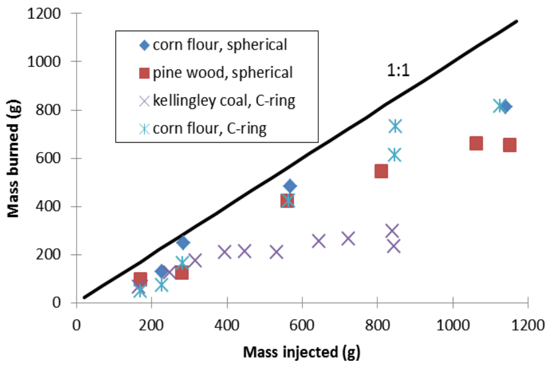

Fig. 10 Mass burned as a function of mass injected in the ISO 1 m^3

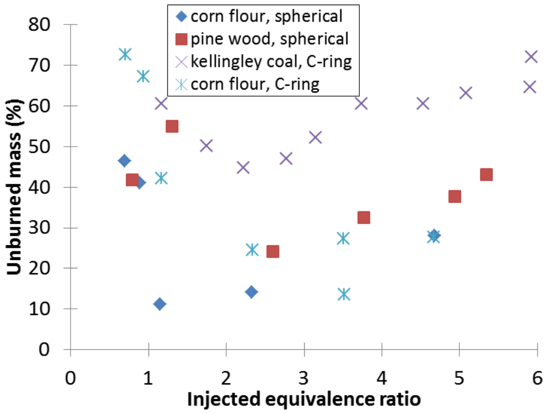

Fig. 11 Unburned mass as a function of injected Ø

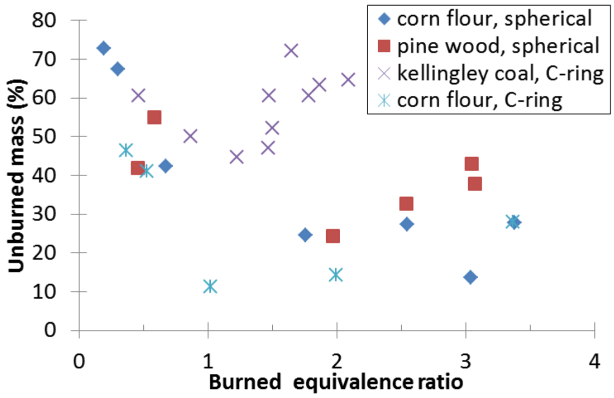

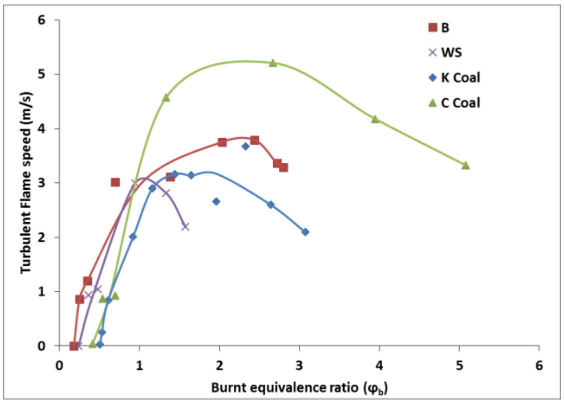

Fig. 12 Unburned mass as a function of the Burnt equivalence ratio, Ø$_{\text{burnt}}$.

Fig. 13 Turbulent spherical flame speed As a function of Ø$_{\text{burnt}}$.

This is normally quite low at <10% of the nominal mass. Fig. 11 shows the unburned mass as a function of the injected equivalence ratio and Fig. 12 shows it as a function of the burnt equivalence ratio. An example of plotting the results of the turbulent flame speen mixture reactivity as a function of the burnt equivalence ratio is shown in Fig. 13, for two coal samples using the standard C ring injector and two biomass samples, bagasse and wheat straw using the spherical grid injector.

These results show the significant effect of the injected dust that does not participate in the explosion on the equivalence ratio through which the flame propagates, Ø$_{\text{burnt}}$. The unburnt mass is at a minimum for the most reactive mixtures, which Fig. 12 shows to be just on the rich side at Ø$_{\text{burnt}}$ = ~ 1.1, which is where the peak reactivity would be for gases. The main reactivity data is plotted later but Fig. 13 shows measured turbulent flame speeds in the 1 m^3 vessel in the constant pressure period and these have a peak value between Ø$_{\text{burnt}}$ of 1 – 2.5 depending on the material. These are more realistic results than those in Fig. 1 with data plotted as a function of the nominal Ø.

Figs. 10-12 show that typically around half of the mass does not burn in an ISO 1m^3 explosion and that the fraction that does not burn increases for mixtures near the MEC and for very rich mixtures. This raises the question of what is the concentration at the MEC. The difficulty is that near the limits of flame propagation the slowly burning flame is acted on by buoyancy and rises up the vessel and quenches on the roof. This occurs in gas explosions as shown by Satter et al. (2012), who showed that at the most reactive mixture near adiabatic flame propagation occurred with negligible flame buoyancy. It was assumed that the same occurred for dust mixtures, so that the quantity of unburnt dust after the explosions was not influenced by incomplete combustion due to flame buoyancy. It was proposed that the fraction of unburnt dust should be kept constant for all dust mixtures to represent the unburnt dust that would occur if there was no buoyancy. All the injected dust concentrations were then corrected on this basis to yield the 'burnt equivalence ratio'. This avoids the situation where the mixture that just burnt at the MEC was ascribed a concentration that was essentially air and thus extremely lean, as near the limit most of the dust does not burn. This shows that the measurement of the dust concentration for limiting flame propagation in the ISO 1 m^3 is difficult, but the MEC cannot be based on the nominal mass injected concentration, as is usually done. The reason for the large unburnt fraction of dust was shown by Satter et al. (2012) and Slatter et al. (2014) to be due to the explosion induced wind ahead of the flame entraining particles and pushing them onto the wall, where they formed a short duration insulating layer, which fell to the floor in most cases after the explosion. This dust did not participate in the flame propagation.

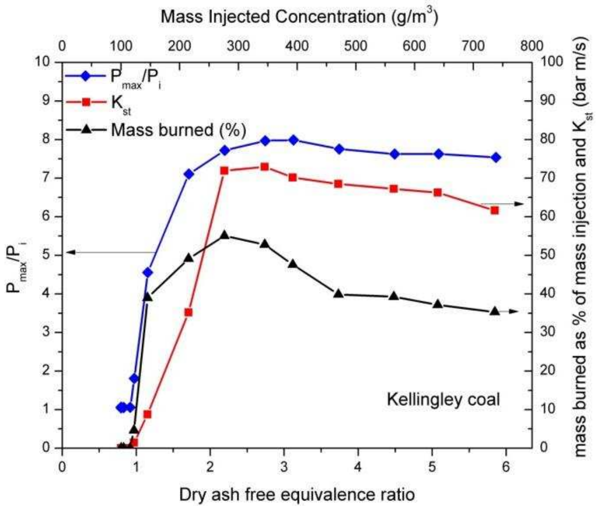

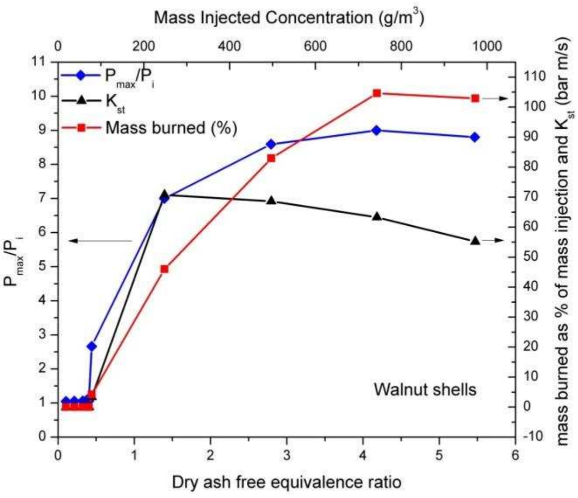

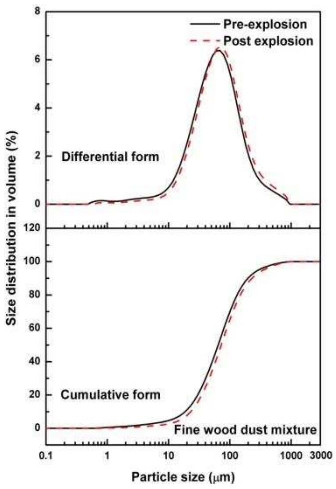

5. MEC data for dusts expressed in equivalence ratio, Ø.

The lean limit is determined by a critical minimum flame temperature for the flame chemistry to be fast enough to sustain a flame [14,15], which will be shown to be 1400K - 1500K. However, the rich limit is much more dependent on the type of hydrocarbon [14,15]. For dusts the rich limit is rarely determined [9] and the lean limit is most commonly only measured as usually no rich limit has been demonstrated and the reasons for this are discussed later.

For many years the lean flammability of gases and vapours was determined using equipment developed at the US Bureau of Mines [14, 15]. This consisted of a 1.5m high vertical tube of 50mm diameter and the limit definition was that the flame with bottom ignition must travel through the vertical tube and emerge at the top i.e. a 1.5m travel distance. Flames that started but quenched part way up the tube were deemed to be not flammable. The measured lean limits, converted to equivalence ratio, are shown in Table 1 for several gases and vapours. For most gas and mist hydrocarbons and alcohols, these are in the equivalence ratio region of 0.45 – 0.64 for gases. A large part of this range is the data for alcohols and most of the hydrocarbon data falls in the lean limit equivalence ratio range of 0.5 – 0.55. This includes data on gasoline, kerosene and diesel mist explosions. This lean limit range converts to a range of critical lean limit temperatures of 1480-1550K [24]. It is considered that to take a lean limit critical temperature of 1500K would be a conservative value in risk analysis, based on the US Bureau of Mines lean limit measurement method. Most existing safety data is based on this lean limit measurement method.

In recent years with the advent of legislation on explosion prevention, standard methods of lean flammability have been developed which must be used for regulatory purposes. In Europe in 2004 [16] the method of measurement that was adopted under the ATEX Directive was based on the German standard method [17] and the EU standard consists of an 80mm diameter vertical tube 300mm long and the definition of the limit is that the flame travels at least 100mm from the spark. The only difference from the German standard is that this used a 60mm diameter tube[17] and both methods give the same results [18,19] The EU and German standard methods result in lean limits for gases and vapours that are leaner than those based on the US Bureau of Mines method, due to the change in definition of the minimum travel distance. The difference in the tube diameter from the US Bureau of Mines 50mm tube is not significant. The 100mm travel distance limit flames, in the EU and German standards, will not travel the 1.5m distance in the US Bureau of Mines equipment and for nearly a century have been rejected as flammable flames [25]. The European standard based lean limits have been published in the standard for four HCs and for a range of hydrocarbons by Schroder and Molnarne [18] and these and those in the standards have been converted into the lean limit equivalence ratio in Table 1. There are similar developments of lean limit standards in the US and these generally give leaner flammability limits than the US Bureau of Mines limits [24].

Lean limit data for the new European standard or its German predecessor have only been published for a few of the compounds in Table 1. However, the lean equivalence ratios for hydrocarbon gases are in the range 0.38 – 0.48, including alcohols and ethylene. If ethylene is excluded the lean limit range for hydrocarbons and alcohols is 0.42 - 0.48 and an average of 0.45 would be reasonable. This corresponds to a critical lean limit flame temperature of 1382K. In view of the uncertainties in the lean limit measurements it would be reasonable to take 1400K as the critical lean limit temperature for most hydrocarbon-air flames using the recent legislation approved lean limit measurement methods. This is 100K lower than was concluded based on lean limit measurements using the US Bureau of Mines equipment.

Andrews et al. [24] have reviewed 11 published measurements of the lean limit for methane-air, all using legislation approved measurement methods in Europe and the US. They concluded that a reasonable mean value was Ø=0.47 (1421K). Andrews and Bradley [26] have also shown for methane-air explosions, that the leanest mixture that a flame can be measured, by high speed laser schlieren interferometry photography, propagating from a spark in a 300mm diameter cylindrical closed vessel, was 4.5% or an equivalence ratio of 0.47. The influence of buoyancy on this slow burning limit flame was to convect it vertically until it quenched on the vessel roof (150mm from the spark), at which stage no significant pressure rise had occurred.

The present authors have also measured the lean flammability limit in a closed explosion vessel that was 1.5m long and 76mm diameter, effectively the US Bureau of Mines equipment operated under closed vessel conditions with bottom ignition and vertical flame propagation [26a]. Using a limit defined by a minimum pressure rise of 0.1bar a lean limit for methane was measured at Φ=0.45 (1382K). This does not mean that the flame travelled 1.5m, but that sufficient flame travel occurred to burn enough mixture to give a significant pressure rise. These two independent measurement techniques support the conclusion from recent legislation approved methods of flammability measurements that the lean limits for hydrocarbon-air explosions is leaner than that in most safety guidance and that a critical lean limit temperature of 1400K would be a reasonable design procedure. Andrews and Bradley [26] measured the burning velocity of the limit flame at Φ=0.45 as 0.05 m/s and that at Φ=0.5 as 0.1 m/s.

For dusts the lean limits in Table 1 have been determined from one of three test vessels: the 1.2L Hartmann vertical cylinder, the 20L sphere and the ISO 1m^3 sphere [9]. All three methods are empirical, in that the method of dispersion of the dust is arbitrary due to the need to generate flow and turbulence to suspend the dust/air mixture. Also, there is an arbitrary ignition delay between injecting the air and dust into the vessels and igniting the mixture. A fixed delay has to be specified in the tests as this determines the turbulence level. There is no approved laminar dust cloud test method, whereas all gas and mist data is for laminar mixtures of fuel and air.

The Hartmann equipment uses a continuous spark as an ignition source and the 20L and 1m^3 spheres use a 10kJ chemical ignitor, which is to ensure that the lean limit is measured and not the spark ignition limit. However, only for a small number of dusts does the Hartmann equipment give lean limits significantly different from the other methods that use a higher ignition energy. The 20L sphere is not ideal for lean limit measurements [4] as the 10kJ chemical ignitor produces a 1bar pressure rise in the small volume with no dust present; this effectively preheats the mixture, which extends the lean limit. The data shown in Table 1 for the lean limit of dusts has come from either the Hartmann equipment in the data compilations of Maisey [22] and Field [23] or from either the 20L or 1m^3 in the large data compilation of Eckhoff [9], which does not distinguish which data came from which experimental equipment. For cellulose and polyethylene dusts in Table 1 measurements exist for both the 1.2L Hartmann and either the 20L or 1m^3 and identical lean limits were found.

All lean flammability results for gases, vapours, mists and dusts can only be compared if they are expressed in terms of their lean limit equivalence ratio, as in Table 1. If there are hybrid mixtures of gases, vapours, mists and dusts then these hybrid mixtures should be evaluated by summating the total mass of gas, vapour, mist and dusts and expressing a total mass A/F ratio. If the type and proportion of gas, vapour, mist and dusts are known then the mean stoichiometry can be evaluated and the overall equivalence ratio determined. There is no need for cumbersome equations for the lean limits of mixtures or for graphical presentation of gas/dust flammability data, as is often done [8, 9]. Thus, a propane mixture with 2% propane by volume in the presence of 20 mg/m^3 of a hydrocarbon dust, both of which are not flammable as individual components will be flammable in combination as each has $\Phi=0.25$ and in combination $\Phi=0.5$ and will be flammable. The stoichiometry of hybrid mixtures of HC and HCO materials can be determined if the proportion of the two materials are known so that the mean stoichiometric composition can be evaluated on an air/fuel ratio by mass basis. The air/fuel ratio of hybrid mixture can then be evaluated and its equivalence ratio determined. If it is >0.45 (European flammability measurement equivalent) then the hybrid mixture should be deemed to be flammable.

The data in Table 1 shows that most hydrocarbon and alcohol gases and mists have the same lean limit equivalence ratio of close to 0.55 for the US Bureau of Mines method or 0.47 for the new European measurement method, for which no mist measurements have been published. For pure hydrocarbon dust explosions such as those for polyethylene and polypropylene, Table 1 shows that they have a lean limit Φ of 0.37 and 0.43, respectively. These are much closer to the new European flammability measurement results for hydrocarbon gases and air. For polyethylene the dust the lean limit is identical to that for gaseous ethylene ($\Phi_{LL}=0.38$), whereas for polypropylene the dust limit at $\Phi_{LL}=0.43$ is significantly leaner than that for gaseous propylene which has $\Phi_{LL} = 0.54$. These results indicate that the solid polyethylene probably decomposes, under the flash heating of flame propagation, to yield ethylene as related oligomers do not have the same flammability limits. However, for polypropylene some decomposition to form the oligomer ethylene is likely as a possible reason for the leaner do not have the same flammability limits. However, for polypropylene some decomposition to form the oligomer ethylene is likely as a possible reason for the leaner lean limit of polypropylene dusts than propylene gas.

For HCO dusts the results are quite unusual, as the lean limit is much leaner in equivalence ratio terms than would be expected based on the results for alcohol vapours, which are very similar to hydrocarbons. For the four pure chemical HCO dusts, the lean limits in Table 1 vary between $\Phi= 0.18$ and 0.24, much leaner than for the pure hydrocarbon dusts. There is very sparse data for lean limits of naturally occurring HCO dusts such as wood dusts. Where the HCO dusts data is available the HCO composition of the dust is not given. Table 1 gives the stoichiometric mixture for a range of biofuels, for which the HCO composition is known but for which no lean flammability data has been reported. Table 1 includes the reported lean limit data for wood dust explosions, for which no HCO composition was given. These results in Table 1 indicate that the lean limit data is compatible with that for pure HCO chemicals and is around $\Phi=0.2$. There is an urgent need for more data on the dust explosion hazards of biofuels, as major plants are under construction for co-firing pulverised wood and straw with coal with no reliable published data on the explosion risk in the dust handling plant.

For agricultural dusts, such as those that occur in grain silos, there is a lot of experimental data of the explosion lean limits but few publications of the HCO composition of the dusts. However, it is likely that their behaviour will be similar to other HCO materials and have a lean limit around $Ø=0.2$. It has previously not been realised that HCO dusts had lean limits at least half those for hydrocarbon gases, mists and dusts in terms of their lean limit equivalence ratios, as the lean limits for dusts have rarely been expressed in equivalence ratio terms.

A feature of the experimental results for HCO dusts in Table 1 is shown when the gas, mist and dust results are compared in the dust measurement units of g/m^3. Table 1 shows that all gaseous fuel have limits of 30-37 g/m^3 for the European lean limit test method. Pure hydrocarbon dusts have lean limits of 30-35 g/m^3 and pure HCO chemicals in dust form have lean limits of 30-40 g/m^3. Also the mean value of the lean limit for wood dusts is 35 g/m^3. There are also many agricultural dusts of HCO elemental composition with lean limits of 30-60 g/m^3 [9, 22]. Taken together, all of these data suggests that, in explosions, solid HCO dusts behave much as hydrocarbons, and this should be contrasted with alcohol vapours which have lean limits of about Φ=0.5 rather than values of about Φ=0.2 associated with most HCO dusts. This difference is considered to be due to the vapour of alcohols having the same chemical composition as the liquid alcohol. However, there is no such material as gaseous wood, nor any form of a pure HCO polymer that exists as a polymer in the vapour form. When HCO solid materials are rapidly heated, as in a dust explosion flame, the first material to be released is hydrocarbons and this is why the lean limit is close to that of hydrocarbons in mass terms rather than the expected lean limit as half the stoichiometric equivalence ratio.

One requirement of the ATEX Directive is that explosion protection must be provided for the worst case explosions scenario, which is that of the most reactive mixture. For gases and vapours this is the mixture with the highest flame temperature, which is close to Φ=1.05. However, for propane and butane the most reactive mixture in large explosions occurs for richer mixtures close to Φ=1.3. This is due to the development of cellular flames which are influenced by mixture Lewis numbers (ratios of conduction to diffusion in the flame front) and result in the maximum flame acceleration due to these effects for rich mixtures. The problem is that for explosion protection data such as venting, which is discussed later, the experimental data has often not been carried out for the most reactive mixture, but has been carried out at the mixture with the highest laminar burning velocity for small flame measurements. As this does not include the cellular flame acceleration effect, the venting guidelines may provide data that are not for the most reactive mixture.

Table 5 Comparison of MEC measured by the Hartmann, 20L and 1 m^3 spheres [Eckhoff, 2003; NFPA68, 2013; Field, 1983; Maisey, 1965]

Dust	Hartmann	1 m^3 or 20 L	1 m^3
Sugar	45	60	60
Milk Powder	50	60	60
Aluminium	30 6 µm 40 17 µm	30 22-29 µm 6 < 10 µm 60 41 µm	30 29 µm
Cellulose	55	60 51 µm	60 33 µm
Wheat Starch	45	60 20 µm	30
Lycopodium This work	22 22		30 14 (burnt)
Polypropylene	30 – 35	30 25 µm	30
Polyethylene This work	30 15 63 µm	30 <10 µm	30 <10 µm
Sulphur	20	30 20 µm	30
Peat	100	60-125	125

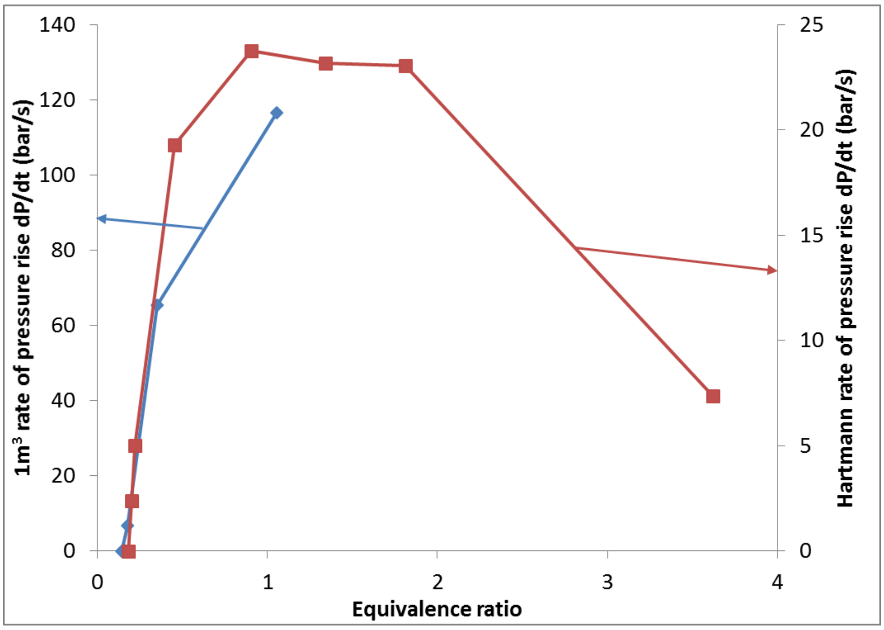

Comparison of rate of pressure rise from 1 m^3 vessel and Hartmann tube measurements against equivalence ratio for fine fraction of steam exploded wood< 63 µm

For dusts the situation is even worse, as the maximum reactivity occurs well on the rich side of stoichiometric. For many dusts the maximum reactivity occurs around 500 g/m^3 [8, 9, 22, 23]. Comparison with Table 1 shows that the most reactive mixture is for Φ ~3-5, which are much richer mixtures than for gases. The reason that many dusts have their most reactive mixture for very rich mixtures has had little comment in the literature and the flame propagation mechanism that gives rise to this is not known. However, it is essential that these very reactive rich mixtures are those for which explosion protection measures are developed.

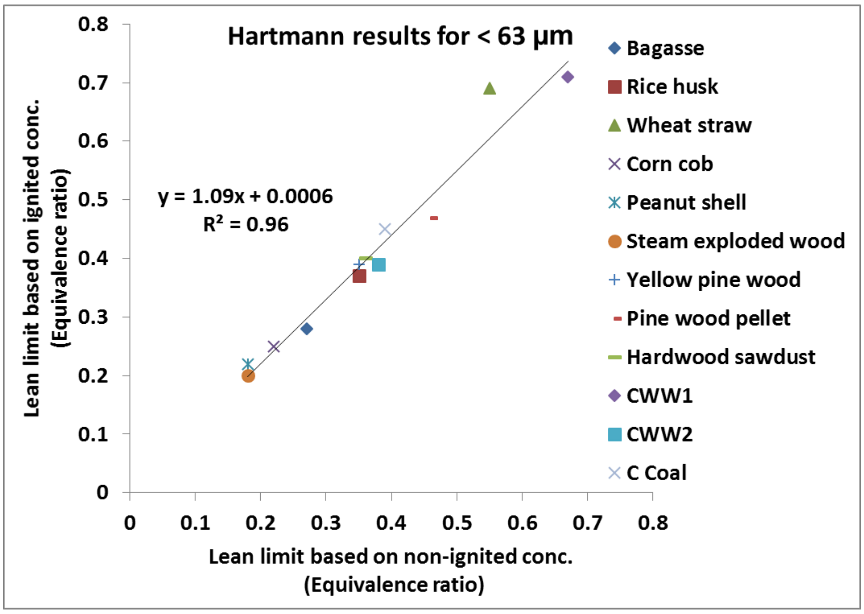

Conclusions

Briefly summarize the main conclusions of the study.

Acknowledgements

The authors gratefully acknowledge the financial support from the EPSRC Energy programme.

References

Andrews, G. E. and Phylaktou, H. N. (2010). Chapter 1.16 Explosion Safety. In: Handbook of Combustion. John Wiley and Sons, Inc., 377–413, DOI: 10.1002/9783527628148.hoc016

Bartknecht, W. (1993) Explosionsschultz, Grundlagen und Anwendung, Springer Verlag.

Eckhoff, R.K. (2003). Dust explosions in the process industries. Gulf Professional Publishing, Amsterdam, third edition.

EN,1839:2003, Limits of Flammability measurement standard for gases and vapours. European Standard BS

Field, P. (1983). Explosibility assessment of industrial powders and dusts, HMSO, Dept. Env., BRE.

Huéscar-Medina, C., Phylaktou, H. N., Sattar, H., Andrews, G. E., & Gibbs, B. M. (2013). The development of an experimental method for the determination of the minimum explosible concentration of biomass powders. Biomass and Bioenergy. doi:10.1016/j.biombioe.2013.03.008

Maisey, H. (1965), Gaseous and dust explosion venting. Chem. Process Eng, p. 527.

NFPA 68 (2013). Explosion Protection by Deflagration Venting. National Fire Protection Association, Batterymarch Park, Quincy, MA.

Saeed, M.A., Andrews, G.E., Phylaktou, H.N. and Gibbs, B.M. (2015a). Global kinetics of the rate of volatile release from biomasses in comparison to coal. 1st Chemistry in Energy Conference, Royal Society of Chemistry. Edinburgh, UK. (Also in Fuel 2016)

Saeed, M.A., Sattar, H., Huescar-Medina, C., Slatter, D. Herath, P., Andrews, G.E., Phylaktou, H.N. and Gibbs, B.M. 2015b. Improvements to the Hartmann Dust Explosion Equipment for MEC Measurements that are Compatible with Gas Lean Limit Measurements. Proc. IAFSS, 10th Asia-Oceania Sumposium on Fire Science and Technology, 10th AOSFST, Tsukuba, Japan.

Sattar, H., Slatter, D.J.F., Andrews, G.E., Gibbs, B.M and Phylaktou, H.N.(2012). Biomass Explosions: Investigation of the Ultra Rich Mixtures that give Peak Reactivity. Proc. of the IX International Seminar on Hazardous Process Materials and Industrial Explosions, Krakow.

Sheng, C and Azevedo, J. (2002) Modeling biomass devolatilization using the chemical percolation devolatilization model for the main components. Proceedings of the Combustion Institute, 29(1), 407-414.

Slatter, D., Andrews, G.E., Huescar-Medina, C., Phylaktou, H.N., Gibbs, B.M. and Satter, H., Biomass explosion residue analysis. Tenth International Symposium on Hazards, Prevention, and Mitigation of Industrial Explosions (XISHPMIE) Bergen, Norway, 10-14 June 2014

Staggs, J.E.J. (1999). Modelling thermal degradation of polymers using single-step first-order kinetics. Fire Safety Journal, 32(1), 17-34.

Tillman, Rossi and Kitto, (1981). Wood Combustion', Academic Press.

Wilén, C., A. et al. (1999). Safe handling of renewable fuels and fuel mixtures. VTT Publications, Finland 394: 1-117.

Wong,D., Huntley, S., Lehmann, B. and Zeeuwen, 2013. Sawmill Wood Dust Sampling, Analysis and Explosibility, Final Report 301007168 FPInnovations.

H. Yang, R. Yan, H. Chen, C. Zheng, D. H. Lee and D. T. Liang, (2006). In-depth investigation of biomass pyrolysis based on three major components: hemicellulose, cellulose and lignin. Energy & Fuels, 20(1), 388-393.
Zabetakis, (1965). Limits of Flammability of Gases and Vapours, US Bureau of Mines Bulletin 627.
M. A. Saeed, G. E. Andrews, H. N. Phylaktou and B. M. Gibbs. Effect of steam exploded treatment on the reactivity of wood sample. in Proceedings of the 8th Int. Conference on Sustainable Energy and Environmental Protection (SEEP2015). 2015. Paisley, Scotland, UK.

11. John Macrae 'An introduction to the study of fuel' p. 20, Elsevier, 1966.
12. Harker and Backhurst, 'Fuel and Energy' Academic Press 1981 p.29.
13, Sjaak van Loo and Jaap Koppejan, 'The Handbook of biomass combustion and co-firing', earthscan, 2008.
14. Coward, H. F., and Jones, G. W., 'Limits of Flammability of Gases and Vapours', US Bureau of Mines, Bulletin 503, 1952
17. BAM, Bestimmung der Explosionsgrenzed von Gases und Gasgemischen in Luft, DIN 51649, Tell 1 ,1986.
18. Schroder and Molnarne, J. Hazardous Materials, A121, 37-44, 2005.
19. Razus et al., Chem. Eng. & Processing Vol. 43 p. 775-784, 2004
20. Barnett and Hibbard (Eds) NACA RM E54107, 1955.
21. Odgers, J and Kretschmer, Gas turbine fuels and their influence on Combustion, Abacus Press, 1986
22. H.R. Maisey, Chemical and Process Engineering, Oct. 1965.
24. Andrews, G.E., Ahmed, N.T., Phylaktou, H.N. and King, P., "Weak Extinction in Low NOx Gas Turbine Combustion". The ASME IGTI International Gas Turbine Congress, ASME Paper GT2009-59830, ISBN 978-0-7918-3849-5, 2009.
25. Coward, H.F. and Brinsley, J. Chem. Soc. Vol.105, p. 1859-1885, 1914.
26. Andrews, G.E. and Bradley, D., Proceedings of the 14th International Combustion Symposium, pp. 1119-1128, 1973.
26a. Phylaktou, H.N., Andrews, G.E. and Herath, P., J. Loss Prevention in the Process Industries, Vol.3, p.355, 1990.
27. Hattwig, M. and Steen, H. (Eds), Handbook of Explosion Prevention and Protection, Wiley-VDH, 2004.

Incomplete paper – see powerpoint version for complete presentation